

# N-a-Acetyltransferase 10 protein inhibits invasion and metastasis of oral squamous cell carcinoma via regulating Pirh2-p53 signaling pathway

**Fazhan Wang**

Key Laboratory of Xinjiang Endemic and Ethnic Disease

**Jun Zheng**

Department of Stomatology, The First Affiliated Hospital, School of Medicine, Shihezi University

**Yongyong Yang**

Department of Urology

**Jie Yang**

Key Laboratory of Xinjiang Endemic and Ethnic Disease

**Ting Luo**

Key Laboratory of Xinjiang Endemic and Ethnic Disease

**Jiang Xu**

Department of Stomatology, The First Affiliated Hospital, School of Medicine, Shihezi University

**Yongqing Gu**

Beijing Key Laboratory for Radiobiology

**Yan Zeng (✉ [zengyan910@gmail.com](mailto:zengyan910@gmail.com))**

Key Laboratory of Xinjiang Endemic and Ethnic Disease & Department of Stomatology

<https://orcid.org/0000-0002-9823-1266>

---

## Research

**Keywords:** Naa10p, OSCC, invasion, Metastasis, Pirh2-p53

**Posted Date:** May 21st, 2020

**DOI:** <https://doi.org/10.21203/rs.3.rs-29042/v1>

**License:**  This work is licensed under a Creative Commons Attribution 4.0 International License.

[Read Full License](#)

---

## **Abstract**

## **Background**

Naa10p (N-a-Acetyltransferase 10 protein) was reported to be involved in tumor invasion and metastasis in several of tumors. However, the role and mechanism of Naa10p mediated invasion and metastasis in oral squamous cell carcinoma (OSCC) remains undetermined.

## **Methods**

The functional role of Naa10p in OSCC cells were determined using Transwell assay in vitro and xenograft tumorigenesis in nude mice. Immunoprecipitation, GST-pull down assays and immunofluorescence were performed to confirm the interaction between Naa10p and RelA/p65 in OSCC cells. Lastly, luciferase reporter assays, chromatin immunoprecipitation (ChIP) and western blot were used to evaluate the effect of Naa10p expression on the Pirh2-p53 signaling pathway.

## **Results**

Naa10p inhibits cell migration and invasion in vitro and attenuates the xenograft tumorigenesis in nude mice. Mechanistically, there is a physical interaction between Naa10p and RelA/p65 in OSCC cells, thereby preventing RelA/p65-mediated transcriptional activation of Pirh2. Consequently, inhibition of Pirh2 increased p53 level and suppressed the expression of p53 downstream targets, MMP-2 and MMP-9.

## **Conclusion**

Naa10p function as a tumor metastasis suppressor in the progression of OSCC by targeting Pirh2-p53 axis, and might be a prognostic marker as well as a therapeutic target for OSCC.

## **Background**

Oral squamous cell carcinoma (OSCC), a subset of head and neck squamous cell carcinoma(HNSCC), is the most prevalent malignant neoplasm of the oral cavity<sup>[1]</sup>, with approximately 300,000 newly diagnosed cases and 170,000 cancer deaths worldwide each year<sup>[2]</sup>. Although substantial development in both the diagnosis and sequential treatment over recent decades, the long-term survival of OSCC patients has not been significantly improved. One of the most common causes that lead to death in OSCC patients is metastasis. The 5-year survival rate with lymph node metastasis is 50%, while the 5-year survival rate with distant metastasis is only 20%<sup>[3]</sup>. However, the molecular mechanism underlying the metastasis of OSCC remains largely unknown.

N- $\alpha$ -Acetyltransferase 10 protein (Naa10p/ARD1), the catalytic subunit of N-terminal acetyltransferase complex (NatA), has both N- $\alpha$  and N- $\epsilon$  acetylation activities<sup>[4–6]</sup>. Naa10p is involved in regulating cell proliferation<sup>[6–8]</sup>, apoptosis<sup>[9, 10]</sup>, autophagy<sup>[11, 12]</sup>, tumor metastasis<sup>[13, 14]</sup> and cell cycle arrest<sup>[15]</sup>. Naa10p overexpression has been documented in breast cancer<sup>[16]</sup>, colorectal cancer<sup>[17]</sup>, hepatocellular cancer<sup>[18]</sup> and lung cancer<sup>[19]</sup>. While downregulation of Naa10p in thyroid neoplasm<sup>[20]</sup> and non-small cell lung cancer (NSCLC)<sup>[11]</sup> was also reported. Although the efforts to elucidate the biological function of Naa10p, it remains disputed regarding its roles in cancer. Naa10p was shown to physically interact with and acetylated the androgen receptor (AR) and form a positive feedback loop for AR-dependent prostate tumorigenesis<sup>[8]</sup>. Moreover, In lung cancer cells, Naa10p potentiates DNMT1's affinities with promoter regions of tumor suppressor gene E-cadherin and LATS, thereby suppressing their transcription and facilitating tumorigenesis<sup>[21]</sup>. Naa10p was also reported to interact with  $\beta$ -catenin and promote transcription of cyclin D1 in lung cancer cells<sup>[6]</sup>. By binding to p65 subunit of nuclear factor- $\kappa$ B (NF- $\kappa$ B), Naa10p may increase MCL1 transcription and resistance to stimuli-induced apoptosis<sup>[10]</sup>. In osteosarcoma, Naa10p was directly associated with MMP-2 protein through its acetyltransferase domain and maintained MMP-2 protein stability via NatA complex activity<sup>[14]</sup>. However, other studies found that Naa10p may serve as a tumor suppressor. By binding to PIX proteins, Naa10p inhibited Cdc42/Rac1 activity and therefore suppressed tumor metastasis<sup>[19]</sup>. Besides, Naa10p inhibits the migration and invasion of breast cancer cells by binding to STAT5a and decreases STAT5a-stimulated ID1 expression<sup>[13]</sup>. TSC2 was found to be acetylated and stabilized by Naa10p, through which Naa10p inhibits mammalian target of rapamycin signaling pathway and suppressed tumorigenesis<sup>[11]</sup>. Naa10p may play diverse roles in different types of cancer cells or different stages during cancer tumorigenesis, and thus identifying cancer-type specific targets will help to understand the role of Naa10p in a certain cancer type<sup>[14]</sup>.

p53 has been shown to be involved in the regulation of cell cycle arrest, DNA damage repair, and apoptosis<sup>[22, 23]</sup>. Of particular interest, the emerging evidence demonstrated that p53 plays a critical role in inhibiting cancer invasion and metastasis<sup>[24, 25]</sup>. Matrix metalloproteinases (MMPs) play an important role in tumor invasion, metastasis and tumor-induced angiogenesis by degrading basement membrane and extracellular matrix (ECM)<sup>[26, 27]</sup>. It has been shown that p53 can potently attenuate the expression of MMP-1<sup>[28]</sup>, MMP-2<sup>[29]</sup>, MMP-9<sup>[30]</sup> and MMP-13<sup>[31]</sup>. Pirh2 is a p53-induced protein, and has been shown to ubiquitylate p53 in vivo and in vitro<sup>[32]</sup>. Indeed, Pirh2, as an oncoprotein, was found to be stabilized and upregulated in several of tumor tissues, including head and neck cancer<sup>[33]</sup>. The overexpression of Pirh2 was concomitant with decreased p53 levels in malignant tissues, suggesting a role for Pirh2 in tumorigenesis through regulation of p53 stability and expression<sup>[34]</sup>.

In previous study, we revealed that the expression of Naa10p was negatively correlated with that of Pirh2 in OSCC tissues. Besides, positive Naa10p and negative Pirh2 might be independent biomarkers for better prognosis in OSCC patients<sup>[35]</sup>. However, the precise mechanism that Naa10p down-regulated Pirh2 remains unknown. Here, we demonstrated that Naa10p has a role in invasion and metastasis in OSCC.

Mechanistically, we elucidated that Naa10p interacts with RelA/p65 in the OSCC cells cytoplasm, and subsequently inhibits RelA/p65-mediated transcriptional activation of Pirh2 by preventing the nuclear translocation of RelA/p65. Consequently, inhibition of Pirh2 increased p53 level, and suppressed expression of p53 downstream targets, MMP-2 and MMP-9. These data revealed that Naa10p may function as a tumor metastasis suppressor in the progression of OSCC by targeting Pirh2-p53 axis, and might be a prognostic marker as well as a therapeutic target for OSCC.

## Methods

### Cell lines, animals and reagents

Human oral squamous cell carcinoma cell lines CAL 27 and SCC-15 were obtained from ATCC and cultured with standard culture conditions. Cell line authentication was performed according to United Kingdom Coordinating Committee on Cancer Research Guidelines every 2–3 months, including mycoplasma test by PCR and measurement of cell proliferation by counting. Female BALB/c nude mice, 6 weeks old, were purchased from the Beijing Laboratory Animal Center (Beijing, China). Primary antibodies used in this study were listed in Supplementary Table S1.

### Plasmids, small interfering RNAs, transfection and stable cell line generation

Human full-length pCMV-RelA/p65 plasmid and the plasmids with silencing and overexpressing Naa10p, shCon/shNaa10p and pcDNA3.1/ pcDNA3.1-Naa10p were kindly donated by professor Chengchao Shou (Peking University Cancer Hospital & Institute). The luciferase plasmid pGL3-Pirh2 was constructed from upstream 1763 bp of the human Pirh2 gene transcription start site to downstream 144 bp of the gene transcription start site (1907 bp). At the same time, pRL-TK Renilla luciferase plasmid was purchased GenePharma. Small interfering RNAs (siRNAs; listed in Supplementary Table S2) were synthesized by GenePharma (Shanghai, China). RNA interference was achieved by transient transfection using 100 nM siRNA plus Lipofectamine 2000 (Invitrogen) for 48 h. The lentiviral vectors LV-Naa10, LV-shNaa10p and LV-NC (control) were from GenePharma. We generated OSCC cells stably silencing and overexpressing Naa10p, according to a previous study<sup>[36]</sup>.

### Western blot

Protein was lysed by using RIPA lysis buffer containing 1% PMSF to extract the total cellular protein. Cell lysates were incubated on ice for 30 min and then centrifuged for 15min at 13,000×g to remove debris. Aliquots of proteins were boiled in 1×loading buffer for 10 min, samples containing 30μg of total proteins were resolved by SDS-PAGE, and proteins transferred to PVDF membrane (Millipore Corporation, USA). Membranes were incubated with primary antibodies overnight at 4°C and appropriate HRP-secondary antibodies for 2h at room temperature. Protein bands were visualized using enhanced chemiluminescence detection (SuperSignal West Femto Maximum Sensitivity Substrate; Thermo Scientific). Images were gathered by Alpha Innotech's FluorChem imaging system. The antibody information was listed in Supplementary Table S1.

## Gene expression microarray and qRT-PCR

RNA was extracted from cells with Trizol reagent (Invitrogen). Gene expression profiles in Naa10-silenced CAL 27 and control cells were examined by using Affymetrix-Gene Chip Human Exon 1.0 ST arrays containing 41 000 transcripts and variants microarray in Shanghai Gene Chem company, and data were deposited in Gene Expression Omnibus databank (<http://www.ncbi.nlm.nih.gov/geo/query/acc.cgi?acc=GSE52723>). After normalization, the fold change expression was calculated. *P* value < 0.05 and the fold change threshold  $\geq 2$  were chosen to identify the statistically significant alterations. Real-time RT-PCR (qRT-PCR) assay were performed following reported procedures.

## Transwell migration and invasion assays

We carried out cell migration and invasion assays according to a previous study<sup>[19]</sup>. Briefly,  $8 \times 10^5$  cells were respectively plated in an uncoated top chamber (Pore size, 8  $\mu\text{m}$ ; Corning, NY) for migration assay, and in a Matrigel (BD Biosciences, Bedford, MA)-coated top chamber for invasion assay. In both assays, cells were incubated in serum-free medium, and medium supplemented with serum was used for a chemoattractant in the lower chamber. After 24h of incubation, the migrating cells on the lower surface of the membrane were fixed with methanol and stained with crystal violet. The number of cells through the membrane was counted under a light microscope ( $\times 100$ , three random fields per well).

## In vivo tumorigenesis in nude mice

For nude mice tumorigenicity assays,  $5 \times 10^6$  indicated cells were injected into 6-week-old BALB/c female nude mice. The length (L) and width (W) of each tumor mass were measured by calipers once a week. Tumor volume was calculated according to the formula: Tumor volume =  $(L \times W^2)/2$ . After the nude mice were sacrificed, the tumors were removed and weighed, then fixed in 10% neutral buffered formalin for 24 hours, embedded in paraffin, sectioned at 6- $\mu\text{m}$  thickness, and for immunohistochemical staining. The animal study was approved by the biomedical ethical committee of First Affiliated Hospital of the Medical College, Shihezi University and performed along with established National Institutes of Health guide for the care and use concordant with the United States guidelines.

## GST-pull-down assays and Immunoprecipitation

Human full-length Naa10p cDNA was cloned into pGEX-5X-3vector, and the recombinant Glutathione-S-transferases (GST)-Naa10p protein was expressed in Escherichia coli and purified with Glutathione Sepharose 4B beads. 2  $\mu\text{g}$  of His- RelA/p65 (ProteinTech Group) was incubated with 2  $\mu\text{g}$  of either GST-Naa10p or GST plus glutathione beads in binding buffer at 4°C overnight, followed by washing with the same buffer for three times. Proteins were boiled in SDS loading buffer and subjected to western blot with anti-His and anti-GST antibodies. For immunoprecipitation, CAL 27 and SCC-15 cells were lysed in Cell lysis buffer (BL509A, Biosharp). Lysates (1 mg total protein) were incubated with anti-RelA/p65 antibody (2  $\mu\text{g}$ ) for 16 h at 4°C followed by a 2 h incubation with 20  $\mu\text{l}$  immobilized Protein A/G Sepharose beads (sc-2003, Santa Cruz, CA), with normal mouse IgG as a negative control. The beads

were washed with lysis buffer for five times, and the immunoprecipitates were examined by western blot using anti-RelA/p65 and anti-Naa10p antibodies.

### **Subcellular fractionation**

CAL 27 and SCC-15 Cells in the logarithmic growth period were harvested and the fractionation of nuclear and cytoplasmic proteins was performed as described previously<sup>[10]</sup>. and the qualities of cytoplasmic and nuclear extracts were, respectively, verified by western blot with antibodies against β-actin and Histone H<sub>3</sub>.

### **Immunofluorescence**

CAL 27 and SCC-15 cells were grown on coverslips and fixed in 4% paraformaldehyde for 30 min at 4°C, followed by permeabilization with 0.5% Triton X-100 in phosphate-buffered saline (PBS) for 5 min and blocked with 3% bovine serum albumin at room temperature for 1 h. Anti-Naa10p antibody and anti-p65 antibody were then applied to the cells overnight at 4°C, followed by washing with PBS/0.1% Triton X-100 and probing with tetramethyl rhodamine isothiocyanate-conjugated anti-rabbit secondary antibody and fluorescein isothiocyanate-conjugated anti-mouse antibody for 45 min at room temperature. After washing, cells were stained with 4',6-diamidino-2-phenylindole and mounted on 50% glycerol/PBS. A Leica SP2 confocal system (Leica Microsystems, Dresden, Germany) was used to observe the localization of Naa10p and RelA/p65.

### **Luciferase reporter assay**

CAL 27 cells cultured in 24-well plates were transfected with the expression vectors for full-length RelA/p65 and shNaa10p plasmid or empty vector together with the reporter plasmid (500 ng/well) and an internal control vector, pRL-TK (Promega) (50 ng/well) by using lipofectamine 2000. After 48 h, the luciferase activity was measured using a dual luciferase reporter assay kit (E1910, Promega) according to the manufacturer's protocol. The firefly luciferase intensity was normalized based on transfection efficiency measured by Renilla luciferase activity.

### **Chromatin immunoprecipitation assay**

Quantitative chromatin immunoprecipitation (qCHIP) was performed as described previously<sup>[10]</sup>. The sequences of specific primers were listed in Supplementary Table S3.

### **Statistical analysis**

All data for each group is derived from three independent replicates of the experiment. Statistically significant differences were evaluated using the Student's t-test was performed using GraphPad Prism 7.0 (La Jolla, CA, USA). A *P* value < 0.05 was considered statistically significant.

## **Results**

## Naa10p has tumor-suppressive function in vitro and in vivo

Our previous study revealed that Naa10 is overexpressed in OSCC tissues, and Naa10p expression correlates to TNM stage and lymph node status. Moreover, our data confirmed that Naa10p expression is associated with better prognosis, suggesting that Naa10p functions as an independent prognostic factor for OSCC patients<sup>[35]</sup>. To further explore the role of Naa10p in OSCC cells, CAL 27 and SCC-15 cells with stable interference of Naa10p expression were generated by lentiviral infection of shRNA targeting Naa10p. As illustrated in Fig. 1A, silencing of Naa10p was confirmed by western blot analysis in the OSCC cell lines (Left panel, Fig. 1A). Next, cell proliferation capacity was assessed by colony forming assay. Notably, Naa10p knockdown resulted in an increased number of colonies compared with cells transfected with control shRNA. Subsequently, we found that knock-down of Naa10p significantly elevated the migration (Fig. 1B) and invasion (Fig. 1C) of CAL 27 and SCC-15 cells by using transwell assay.

Next, we evaluated the potential effects of Naa10p on tumorigenicity in BALB/c nude mice. Specifically, the growth rates of tumor xenografts were elevated by stable knockdown of Naa10p (Fig. 1D, 1E and 1F). Consequently, mice inoculated with Naa10p-silenced cells had shorter survival time (Fig. 1G). Taken together, these data indicated that Naa10p suppresses tumorigenesis and progression of OSCC in vitro and in vivo.

## Naa10p knockdown inhibits P53 signaling pathway

After elucidating Naa10p's inhibitory roles on OSCC, we sought to further gain insight into the mechanism by which Naa10p regulates invasion and metastasis phenotype in OSCC. We performed cellular Gene Expression Profile with Naa10p stably silenced CAL27 cells and control cells, and the differentially regulated genes were selected for KEGG pathway analysis. The analysis result showed that the P53 signaling pathway was the most relevant downstream signaling pathway of Naa10p (Fig. 2A). Next, we performed Gene Set Enrichment Analysis (GSEA) and found that P53 signaling pathway was enriched in this dataset (Fig. 2B). Subsequently, we performed the genetic variations of P53 signaling pathways of clustering Analysis (Fig. 2C). Consequently, some genes in P53 signaling pathway were determined by qRT-PCR, and Pirh2 was upregulated and p53 downregulated after knocking down Naa10p (Fig. 2D). p53 is a major substrate of Pirh2, and Pirh2 promotes p53 degradation<sup>[32]</sup>. Furthermore, we previously demonstrated that the expression of Naa10p was negatively correlated with that of Pirh2 in OSCC<sup>[35]</sup>. Therefore, the Pirh2-p53 signaling pathway is selected for verification and study in the next step.

## Naa10p attenuates MMPs expression via the Pirh2-p53 signaling pathway

To uncover whether Naa10p was involved in regulating P53 signaling pathway, we verified the expression correlation of Naa10p, Pirh2 and p53 by immunohistochemical staining, which suggested that Naa10p abundance was negatively associated with that of Pirh2, but positively associated with that of p53 (Fig. 3A). Moreover, tumor invasion is often associated with the enhanced synthesis of matrix metalloproteinases (MMPs), among which MMP-2 and MMP-9 are of central importance<sup>[37]</sup>. Thus, we

sought to determine the expression level of Pirh2, p53, MMP-2 and MMP-9 protein in CAL 27 and SCC-15 cells after silencing Naa10p. Western blot showed that Naa10p stable knockdown significantly increased Pirh2, MMP-2 and MMP-9 expression, and decreased p53 expression. Consistently, Naa10p stable overexpression inhibited the level of Pirh2, MMP-2 and MMP-9, and elevated p53 expression (Fig. 3B).

To confirm whether Pirh2 inhibited the expression of p53 and modulated p53-dependent expression of MMPs in OSCC cells, the expression of Pirh2 in OSCC cells was silenced by RNA interference (RNAi). The result showed that Pirh2 knockdown could dramatically increase p53 and decrease MMP-2 in CAL 27 and SCC-15 cells (Fig. 3C). These results emphasized the important role of Naa10p in the p53 pathway and suggested that Naa10p induces Pirh2 reduction and rescues p53 expression.

### **Naa10p interacts with RelA/p65 and attenuates phosphorylation of p65 in OSCC**

In the previous study, there was a significantly inverse correlation of the expression of Naa10p and Pirh2 in OSCC patient tissues<sup>[35]</sup>. Furthermore, the effect of Naa10p on the expression of Pirh2 was determined by qRT-PCR in OSCC cells. The results indicated that Naa10 down-regulates the mRNA expression of Pirh2. (Fig. S1). These data raised a possibility that Naa10p regulates Pirh2 expression at the transcriptional level. Accumulating evidence demonstrated that Naa10p interacts with various transcription factors to regulate the expression of tumor-related target genes<sup>[10,11,13]</sup>. Interestingly, we scanned the proximal 1907bp of the promoter region of Pirh2 using Promo software ([http://alggen.lsi.upc.es/cgi-bin/promo\\_v3/promo/promoit.cgi?dirDB=TF\\_8.3](http://alggen.lsi.upc.es/cgi-bin/promo_v3/promo/promoit.cgi?dirDB=TF_8.3)) and identified potential RelA/p65 binding sites. Thus, we concluded whether RelA/p65 has a transcriptional activation effect on Pirh2 and Naa10p suppresses RelA/p65-mediated transcription by interacting with the RelA/p65. Immunoprecipitation assays were performed to uncover the interaction between Naa10p with RelA/p65 in OSCC cells, and the results revealed endogenous interaction between Naa10p and RelA/p65 in OSCC cells (Fig. 4A). To further investigate the subcellular interaction of Naa10p and RelA/p65, CAL 27 and SCC15 cells were fractionated to acquire cytoplasmic and nuclear proteins. Next, we performed immunoprecipitation assay with cytoplasmic and nuclear proteins and demonstrated the presence of physical interaction was mainly in the cytoplasm (Fig. 4B). In vitro GST-Pull Down assay confirmed the association between GST-tagged Naa10p and His-RelA/p65, indicating a direct binding between these two molecules (Fig. 4C). By immunofluorescence staining and confocal microscopic observation, colocalization of Naa10p and p65 in CAL 27 and SCC-15 cells was revealed mainly in the cytoplasm (Fig. 4D).

Next, we sought to analyze whether Naa10p could affect the level of p65 and p65 phosphorylation. Naa10p was knockdown in CAL 27 cells through shRNA transfection. The results showed that knockdown of Naa10p significantly elevated p65 phosphorylation (serine-536), while p65 did not change (Fig. 4E). Similar results could be observed in SCC-15 cells (Fig. 4E).

### **Naa10p suppresses RelA/p65 activates Pirh2 transcription**

Next, we explored whether RelA/p65 can affect the transcription of Pirh2, the human Pirh2 promoter-luciferase plasmid pGL3-Pirh2 and the RelA/p65 overexpression plasmid were cotransfected to CAL 27 cells, and the transcriptional activation was detected. The luciferase activity was significantly higher than in the control group after RelA/p65 overexpression (Lanes 1 and 3 in Left and Right panels; Fig. 5A). The result elucidated that RelA/p65 has a transcriptional activation effect on Pirh2. Furthermore, we showed that overexpression of RelA/p65 augmented Pirh2's promoter activity, which was enhanced by silencing of Naa10p, but was compromised by co-expression of Naa10p (Lane 3 and 4 in Left and Right panels; Fig. 5A), indicating Naa10p could alleviate RelA/p65-regulated Pirh2 transcription.

To elucidate the RelA/p65 and Pirh2 promoter-specific binding sites, the truncated luciferase reporter plasmid: S1: pGL3-Pirh2-S1 (-1383 ~ +144); S2: pGL3-Pirh2-S2 (-916 ~ +144) of the core segment of the human Pirh2 promoter (length 1907bp) was further constructed based on identified three potential RelA/p65 binding sites on the promoter region of Pirh2 by using Promo software (Fig. 5B). Then, the truncated luciferase reporter plasmids were cotransfected to CAL 27 cells with p65 overexpression plasmid and Naa10p knockdown or overexpressin plasmid, respectively. The results showed that the luciferase activity of the full-length Pirh2 promoter region was increased following Naa10p knokdown and decreased after the Naa10p overexpression. Moreover, the luciferase activity of the truncated Pirh2 promoter regin-S1 was also increased after Naa10p knockdown and is comparable with the full-length Pirh2 promoter. However, the luciferase activity of the truncated S2 had no significant difference with that of the control group (Fig. 5C). Similar data could be observed following stable expression of Naa10p (Right panel, Fig. 5C).

We performed chromatin immunoprecipitation (ChIP)-qPCR assays in CAL 27 cells, and the results revealed that p65 bound to S1 site, but not to S2 site in qCHIP assays (Fig. 5D, Left panel). Once Naa10p was knockdown, binding of RelA/p65 to S1 site was dramatically increased (Fig. 5D, Right panel), suggesting that binding of RelA/p65 to S1 site was negatively regulated by the cellular levels of Naa10p. Collectively, these data indicated that RelA/p65 binds to the promoter region S1 to regulate Pirh2 transcription and Naa10p suppresses RelA/p65 induced Pirh2 transcription.

### The tumor suppressor function of Naa10p is dependent on Pirh2-p53 signaling pathway

To further confirm the migration and invasion effect of Naa10p on OSCC is dependent on the Pirh2-p53 signaling pathway, CAL 27 cells were transfected with Naa10p siRNA or Pirh2 siRNA, respectively or in combination. Notably, silencing of Naa10p promoted CAL 27 cells migration, invasion, and while silencing of Pirh2 inhibited CAL 27 cells migration, invasion. Pirh2 silencing indeed relieved the cell migration and invasion promoted by Naa10p knockdown (Fig. 6A). Similar results were also observed in cell invasion (Fig. 6B). These data suggested that Naa10p functions in the migration and invasion of OSCC cells by targeting Pirh2-p53 signaling pathway.

## Discussion

In this study, we demonstrated the interaction between RelA/p65 subunit of NF-κB with Naa10p, and Naa10p suppressed Pirh2 expression via RelA/p65 dependent transcription in OSCC cells. Pirh2 is a Ring-H2 domain containing E3 ubiquitin ligase, which targets several suppressors genes including p53<sup>[32]</sup>. Emerging evidence further confirmed that Pirh2 might be a novel critical oncoprotein in the development and progression of tumor. Overexpression of Pirh2 had been found in various cancers, including head and neck squamous cell carcinoma (HNSCC). And, Pirh2 expression was correlated with poor prognosis, at least partially through degradation of p27 in HNSCC<sup>[33]</sup>.

The emerging evidence demonstrated that p53 plays an important role in inhibiting tumor invasion and metastasis by regulating the expression and activity of Matrix metalloproteinases (MMPs)<sup>[24,25,28,31]</sup>. Recently, Lee et al. found that p53 is implicated in the regulation on EMT process, and p53 inhibits the expression of E-cadherin and increases that of Snail in OSCC cells. Moreover, p53 inhibited the invasion of OSCC cells via the suppression of MMP-13 expression<sup>[31]</sup>. However, p53 has been shown to be ubiquitylated by Pirh2 in vitro and in vivo, and overexpression of Pirh2 decreased p53 levels and suppressed p53-dependent transactivation and biological function<sup>[34]</sup>. Indeed, the overexpression of Pirh2 was concomitant with decreased p53 levels in malignant tissues, suggesting a role for Pirh2 in tumorigenesis through regulation of p53 stability. Abrogation of Pirh2 results in a steady increase in p53 cellular levels<sup>[34]</sup>. Consistently, we found that the enhancement of p53 inhibited the expression of MMP-2 in CAL 27 and SCC-15 cells after Pirh2 silencing (Fig. 3C). These data provide evidence, Pirh2 promotes tumor invasion and metastasis through suppressing p53.

In the present study, we found that Naa10p inhibits migration, invasion of OSCC cells, and attenuates xenograft tumorigenesis in vivo. Mechanistically, Naa10p decreases Pirh2 expression, and thus it rescues p53 expression and decreases the expression of MMP-2 and MMP-9 to block migration and invasion of OSCC cells. We previously found that the expression of Naa10p was negatively correlated with that of Pirh2 in OSCC tissues. Besides, positive Naa10p and negative Pirh2 might be independent biomarkers for better prognosis in OSCC patients<sup>[35]</sup>. Furthermore, the effect of Naa10 on the expression of Pirh2 was determined by qRT-PCR in OSCC cells. The results indicated that Naa10 down-regulates the mRNA expression of Pirh2 (Fig. S1), suggesting a possibility that Naa10p regulates Pirh2 expression at the transcriptional level. NF-κB is a critical transcription factor activated in various types of human cancers and plays a crucial role in tumor development and progression by inducing transcription of various target genes that modulate cell invasion, proliferation, apoptosis, survival and angiogenesis<sup>[10,38,39]</sup>. We previously discovered that Naa10p interacted with RelA/p65 in Colon cancer cell lines and lung cancer cell lines<sup>[10]</sup> and now we further found that Naa10p interacts with RelA/p65 mainly in the cytoplasm and attenuates phosphorylation of p65 (Serine-536) in OSCC cells. Interestingly, p65 phosphorylated on serine536 translocated to the nucleus following activation, and this nuclear translocation is not regulated by IκBα<sup>[40]</sup>. Here, we hypothesized that Naa10p interacts with p65 in the cytoplasm to inhibit p65 translocation from cytoplasm into the nucleus, resulting in suppressed activation of NF-κB, and thereby inhibiting Pirh2 transcription in OSCC cells. However, our results did not elucidate the mechanism that Naa10p regulates the phosphorylation of p65. Phosphorylation of p65 is an important active form, which

is regulated by various kinases and phosphatases. Activation of IKK kinase leads to phosphorylation of I $\kappa$ B $\alpha$ , which is separated from the p65-p50 complex, and then p65 enters the nucleus and functions as a transcription factor<sup>[41]</sup>. Whether the inhibition of p65 phosphorylation by Naa10p in OSCC cells is dependent on the IKKs deserves further studies.

Based on above results, we speculated whether RelA/p65 has a transcriptional activation effect on Pirh2, and Naa10p suppresses RelA/p65-mediated transcription activity of Pirh2. Therefore, we constructed the luciferase plasmid of the Pirh2 promoter region and detected the transcriptional activation of Pirh2 by RelA/p65 by using luciferase reporter assay. Our result showed that RelA/p65 binds to Pirh2 promoter to regulate its transcription, and Naa10p suppresses RelA/p65 binds to Pirh2 promoter, thus inhibiting Pirh2 expression. Hua et al.'s study reported Naa10p decreases GIT-assisted localization of PIX on membrane protrusions, thus alleviating CDC42/ RAC1-dependent cell metastasis<sup>[19]</sup>. In addition, Lee et al. found silencing of Naa10p resulted in diminished recruitment of DNMT1 to E-cadherin promoter in qCHIP assay, but silencing DNMT1 had no effects on Naa10p's binding to the same site. They also showed that Naa10p could stabilize DNMT1-DNA association by interaction with both non-methylated and hemimethylated DNA<sup>[21]</sup>.

Taken together, this study elucidated that Naa10p, as a tumor suppressor, inhibited tumorigenesis, migration and invasion in OSCC. Mechanically, we demonstrated that Naa10p suppressed RelA/p65-mediated the transcription of Pirh2, and decreased its expression. Therefore, Naa10p elevated p53 protein expression and stability via impairing the effect of Pirh2 on p53 protein degradation, and thus inhibited p53 down-stream genes expression involved in migration and invasion of tumor, such as MMP-2 and MMP-9 (Fig. 7). Our study suggested, Naa10p may serve as a therapeutic target for the prevention of metastasis in OSCC.

## Conclusions

In summary, our findings enriched the role of Naa10p in tumor invasion and metastasis. Naa10p inhibited migration, invasion of OSCC cells, and attenuated tumor xenograft tumorigenesis by interacting with RelA/p65 and inhibiting Pirh2 transcription expression, and subsequently enhancing p53 expression and decreasing the expression of MMP-2 and MMP-9 in OSCC. Naa10p has the potential to become a therapeutic target for the prevention of metastasis in OSCC.

## Abbreviations

Naa10p: N-a-Acetyltransferase 10 protein; OSCC: Oral squamous cell carcinoma; MMP-2: Matrix metalloproteinases 2; MMP-9: Matrix metalloproteinases 9; CHIP: chromatin immunoprecipitation; PBS: phosphate-buffered saline; DAPI: 4',6-diamidino-2-phenylindole; NF- $\kappa$ B: nuclear factor- $\kappa$ B; qCHIP: Quantitative chromatin immunoprecipitation; HNSCC: head and neck squamous cell carcinoma.

## Declarations

## Acknowledgements

We appreciate professor Chengchao Shou (Peking University Cancer Hospital & Institute) for providing the plasmids and antibody.

## Funding

This study was supported by grants 81560473 and 81560442 from National Natural Science Foundation of China, grants 2018CB002 from Xinjiang Production and Construction Corps Key Areas Innovation Team Project, and grants GJHZ201901 from Shihezi University International Cooperation Project.

## Authors' contributions

YZ and YG designed the study. FW, JY and TL performed the experiments. JZ and JX collected the data. FW and JZ analyzed and interpreted the data. FW, JZ and YY prepared the manuscript. All the authors read and approve the final manuscript.

## Availability of data and materials

All data generated or analyzed during this study are included in this published article and its additional files.

## Ethics approval and consent to participate

The animal experiment was approved by the biomedical ethical committee of First Affiliated Hospital of the Medical College, Shihezi University and performed along with established National Institutes of Health guide for the care and use concordant with the United States guidelines.

## Consent for publication

Not applicable.

## Competing interests

The authors declare that they have no competing interests.

## References

1. Shih CH, Chang YJ, Huang WC, Jang TH, Kung HJ, Wang WC, et al. EZH2-mediated upregulation of ROS1 oncogene promotes oral cancer metastasis. *Oncogene*. 2017;36:6542–54.
2. Ferlay J, Colombet M, Soerjomataram I, Mathers C, Parkin DM, Piñeros M, et al. Estimating the global cancer incidence and mortality in 2018: GLOBOCAN sources and methods. *Int J Cancer*. 2019;144:1941–53.

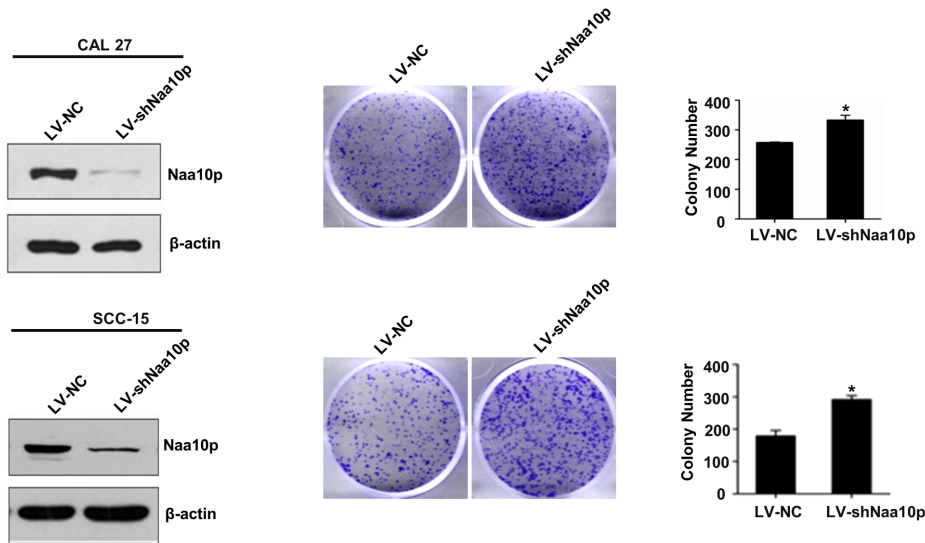
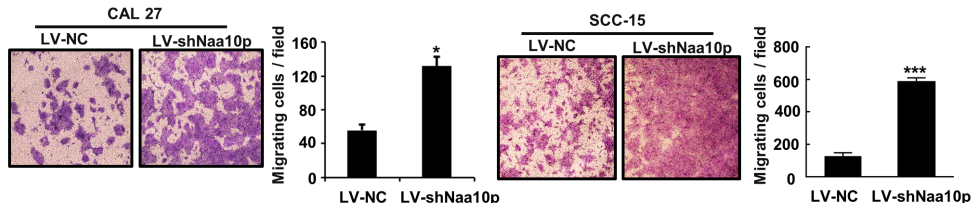
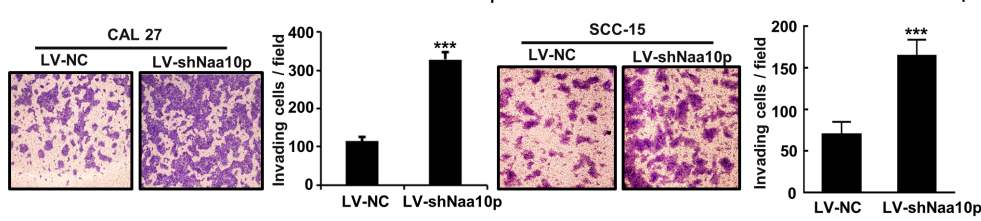
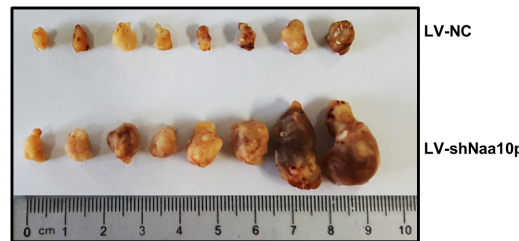
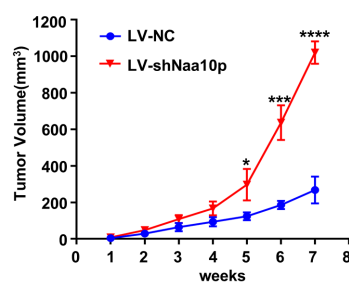
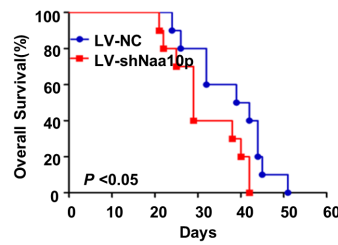
3. Koch FP, Kunkel M, Biesterfeld S, Wagner W. Diagnostic efficiency of differentiating small cancerous and precancerous lesions using mucosal brush smears of the oral cavity—a prospective and blinded study. *Clin Oral Investig.* 2011;15:763–9.
4. Kalvik TV, Arnesen T. Protein N-terminal acetyltransferases in cancer. *Oncogene.* 2013;32:269–76.
5. Seo JH, Park JH, Lee EJ, Vo TT, Choi H, Kim JY, et al. ARD1-mediated Hsp70 acetylation balances stress-induced protein refolding and degradation. *Nat Commun.* 2016;7:12882.
6. Lim JH, Park JW, Chun YS. Human arrest defective 1 acetylates and activates beta-catenin, promoting lung cancer cell proliferation. *Cancer Res.* 2006;66:10677–82.
7. Seo JH, Cha JH, Park JH, Jeong CH, Park ZY, Lee HS, et al. Arrest defective 1 autoacetylation is a critical step in its ability to stimulate cancer cell proliferation. *Cancer Res.* 2010;70:4422–32.
8. Wang Z, Wang Z, Guo J, Li Y, Bavaria JH, Qian C, et al. Inactivation of androgen-induced regulator ARD1 inhibits androgen receptor acetylation and prostate tumorigenesis. *Proc Natl Acad Sci USA.* 2012;109:3053–8.
9. Arnesen T, Gromyko D, Pendino F, Ryningen A, Varhaug JE, Lillehaug JR. Induction of apoptosis in human cells by RNAi-mediated knockdown of hARD1 and NATH, components of the protein N-alpha-acetyltransferase complex. *Oncogene.* 2006;25:4350–60.
10. Xu H, Jiang B, Meng L, Ren T, Zeng Y, Wu J, et al. N-alpha-acetyltransferase 10 protein inhibits apoptosis through RelA/p65-regulated MCL1 expression. *Carcinogenesis.* 2012;33:1193–202.
11. Kuo HP, Lee DF, Chen CT, Liu M, Chou CK, Lee HJ, et al. ARD1 stabilization of TSC2 suppresses tumorigenesis through the mTOR signaling pathway. *Sci Signal.* 2010;3:ra9.
12. Zhang Y, Zhou H, Tao Y, Liu X, Yuan Z, Nie C. ARD1 contributes to IKKbeta-mediated breast cancer tumorigenesis. *Cell Death Dis.* 2018;9:860.
13. Zeng Y, Min L, Han Y, Meng L, Liu C, Xie Y, et al. Inhibition of STAT5a by Naa10p contributes to decreased breast cancer metastasis. *Carcinogenesis.* 2014;35:2244–53.
14. Chien MH, Lee WJ, Yang YC, Tan P, Pan KF, Liu YC, et al. N-alpha-acetyltransferase 10 protein promotes metastasis by stabilizing matrix metalloproteinase-2 protein in human osteosarcomas. *Cancer Lett.* 2018;433:86–98.
15. Gromyko D, Arnesen T, Ryningen A, Varhaug JE, Lillehaug JR. Depletion of the human Nalpha-terminal acetyltransferase A induces p53-dependent apoptosis and p53-independent growth inhibition. *Int J Cancer.* 2010;127:2777–89.
16. Yu M, Ma M, Huang C, Yang H, Lai J, Yan S, et al. Correlation of expression of human arrest-defective-1 (hARD1) protein with breast cancer. *Cancer Invest.* 2009;27:978–83.
17. Jiang B, Ren T, Dong B, Qu L, Jin G, Li J, et al. Peptide mimic isolated by autoantibody reveals human arrest defective 1 overexpression is associated with poor prognosis for colon cancer patients. *Am J Pathol.* 2010;177:1095–103.
18. Midorikawa Y, Tsutsumi S, Taniguchi H, Ishii M, Kobune Y, Kodama T, et al. Identification of genes associated with dedifferentiation of hepatocellular carcinoma with expression profiling analysis. *Jpn*

J Cancer Res. 2002;93:636–43.

19. Hua KT, Tan CT, Johansson G, Lee JM, Yang PW, Lu HY, et al. N-alpha-acetyltransferase 10 protein suppresses cancer cell metastasis by binding PIX proteins and inhibiting Cdc42/Rac1 activity. *Cancer Cell*. 2011;19:218–31.
20. Arnesen T, Anderson D, Baldersheim C, Lanotte M, Varhaug JE, Lillehaug JR. Identification and characterization of the human ARD1-NATH protein acetyltransferase complex. *Biochem J*. 2005;386:433–43.
21. Lee CF, Ou DS, Lee SB, Chang LH, Lin RK, Li YS, et al. hNaa10p contributes to tumorigenesis by facilitating DNMT1-mediated tumor suppressor gene silencing. *J Clin Invest*. 2010;120:2920–30.
22. Levine AJ. p53, the cellular gatekeeper for growth and division. *cell* 1997; 88: 323 – 31.
23. Haffner R, Oren M. Biochemical properties and biological effects of p53. *Curr Opin Genet Dev*. 1995;5:84–90.
24. Sankpal NV, Willman MW, Fleming TP, Mayfield JD, Gillanders WE. Transcriptional repression of epithelial cell adhesion molecule contributes to p53 control of breast cancer invasion. *Cancer Res*. 2009;69:753–7.
25. Hwang CI, Matoso A, Corney DC, Flesken-Nikitin A, Korner S, Wang W, et al. Wild-type p53 controls cell motility and invasion by dual regulation of MET expression. *Proc Natl Acad Sci USA*. 2011;108:14240–5.
26. Westermark J, Kähäri VM. Regulation of matrix metalloproteinase expression in tumor invasion. *Faseb J*. 1999;13:781–92.
27. Shuman Moss LA, Jensen-Taubman S, Stetler-Stevenson WG. Matrix metalloproteinases: changing roles in tumor progression and metastasis. *Am J Pathol*. 2012;181:1895–9.
28. Sun Y, Sun Y, Wenger L, Rutter JL, Brinckerhoff CE, Cheung HS. p53 down-regulates human matrix metalloproteinase-1 (Collagenase-1) gene expression. *J Biol Chem*. 1999;274:11535–40.
29. Wang Y, Zhang YX, Kong CZ, Zhang Z, Zhu YY. Loss of P53 facilitates invasion and metastasis of prostate cancer cells. *Mol Cell Biochem*. 2013;384:121–7.
30. Meyer E, Vollmer JY, Bovey R, Stamenkovic I. Matrix metalloproteinases 9 and 10 inhibit protein kinase C-potentiated, p53-mediated apoptosis. *Cancer Res*. 2005;65:4261–72.
31. Ala-aho R, Grénman R, Seth P, Kähäri V-M. Adenoviral delivery of p53 gene suppresses expression of collagenase-3 (MMP-13) in squamous carcinoma cells. *Oncogene*. 2002;21:1187–95.
32. Leng RP, Lin Y, Ma W, Wu H, Lemmers B, Chung S, et al. Pirh2, a p53-induced ubiquitin-protein ligase, promotes p53 degradation. *Cell*. 2003;112:779–91.
33. Shimada M, Kitagawa K, Dobashi Y, Isobe T, Hattori T, Uchida C, et al. High expression of Pirh2, an E3 ligase for p27, is associated with low expression of p27 and poor prognosis in head and neck cancers. *Cancer Sci*. 2009;100:866–72.
34. Duan W, Gao L, Druhan LJ, Zhu WG, Morrison C, Otterson GA, et al. Expression of Pirh2, a Newly Identified Ubiquitin Protein Ligase, in Lung Cancer. *J Natl Cancer Inst*. 2004;96:1718–21.

35. Zheng J, Wang F, Yang Y, Xu J, Yang J, Wang K, et al. Inverse correlation between Naa10p and Pirh2 expression and the combined prognostic value in oral squamous cell carcinoma patients. *J Oral Pathol Med.* 2019;48:686–95.
36. Zeng Y, Zheng J, Zhao J, Jia PR, Yang Y, Yang GJ, et al. High expression of Naa10p associates with lymph node metastasis and predicts favorable prognosis of oral squamous cell carcinoma. *Tumor Biol.* 2016;37:6719–28.
37. Stetler-Stevenson WG. Matrix metalloproteinases in angiogenesis: a moving target for therapeutic intervention. *J Clin Invest.* 1999;103:1237–41.
38. Kim YR, Kim IJ, Kang TW, Choi C, Kim KK, Kim MS, et al. HOXB13 downregulates intracellular zinc and increases NF-kappaB signaling to promote prostate cancer metastasis. *Oncogene.* 2014;33:4558–67.
39. Jiang L, Lin C, Song L, Wu J, Chen B, Ying Z, et al. MicroRNA-30e\* promotes human glioma cell invasiveness in an orthotopic xenotransplantation model by disrupting the NF-kappaB/IkappaBalpha negative feedback loop. *J Clin Invest.* 2012;122:33–47.
40. Sasaki CY, Barberi TJ, Ghosh P, Longo DL. Phosphorylation of RelA/p65 on serine 536 defines an IkappaB alpha-independent NF-kappaB pathway. *J Biol Chem.* 2005;280:34538–47.
41. Chen ZJ. Ubiquitination in signaling to and activation of IKK. *Immunol Rev.* 2012;246:95–106.

## Figures

**a****b****c****d****e****g****Figure 1**

Silencing of Naa10p promotes OSCC cell migration and invasion, and tumorigenesis in vivo. (a) Stable silencing of Naa10p was examined by Western blot in CAL 27 and SCC-15 cells, and proliferation in CAL 27 and SCC-15 cells after Silencing of Naa10p was assessed by colony forming assay. Colonies were stained with crystal violet 10 days after seeding. (b) and (c) Transwell assay were performed to evaluate the effect of Naa10p silencing on migration (b) and invasion (c) of CAL 27 and SCC-15 cells. (d-f)

Macrograph, volume and weight of tumors in both two groups. (g) Percentage survival of nude mice inoculated with indicated cancer cells. \*P < 0.05, \*\*P < 0.01, \*\*\*P<0.005, as determined by Student's t-test.

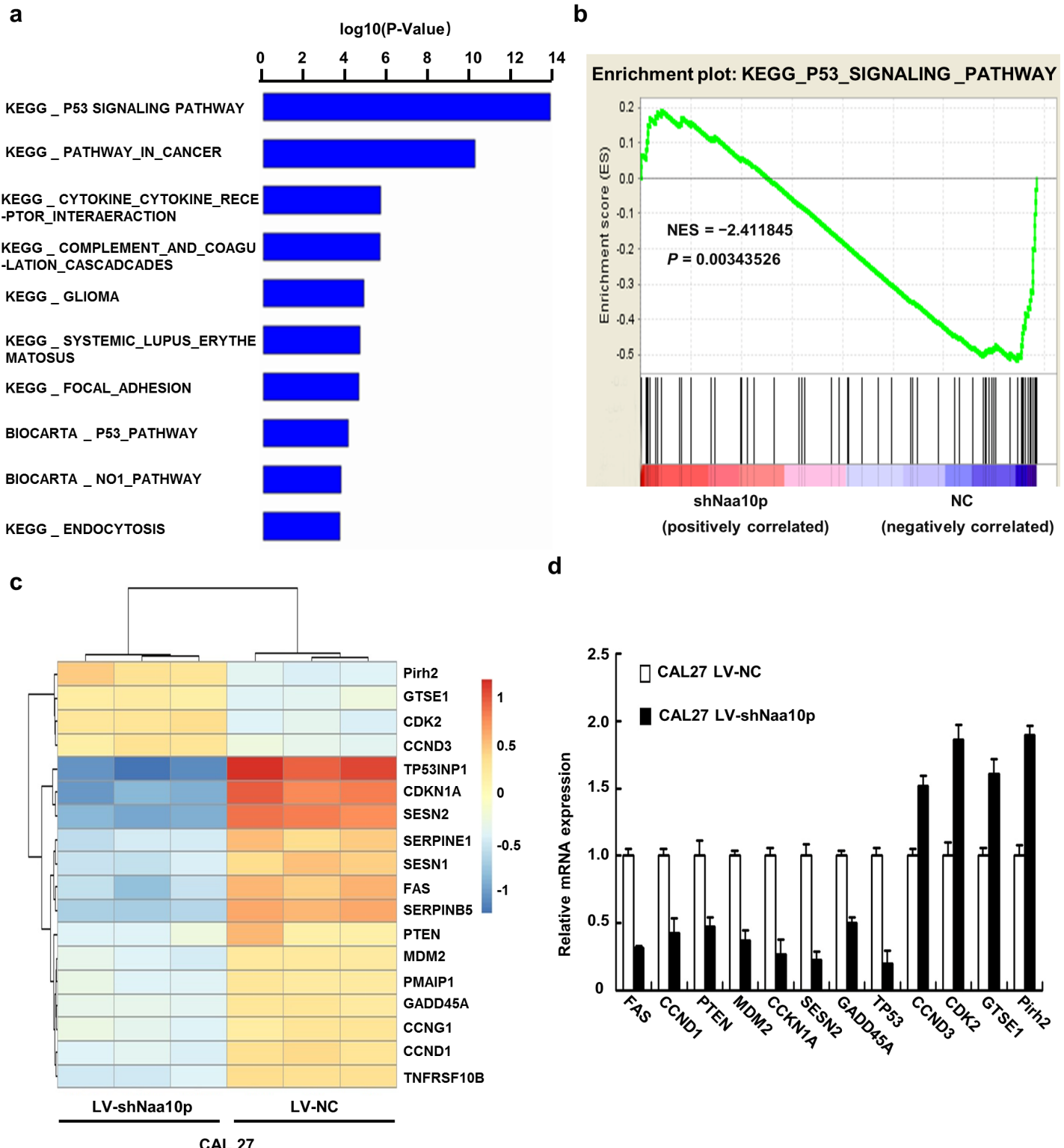
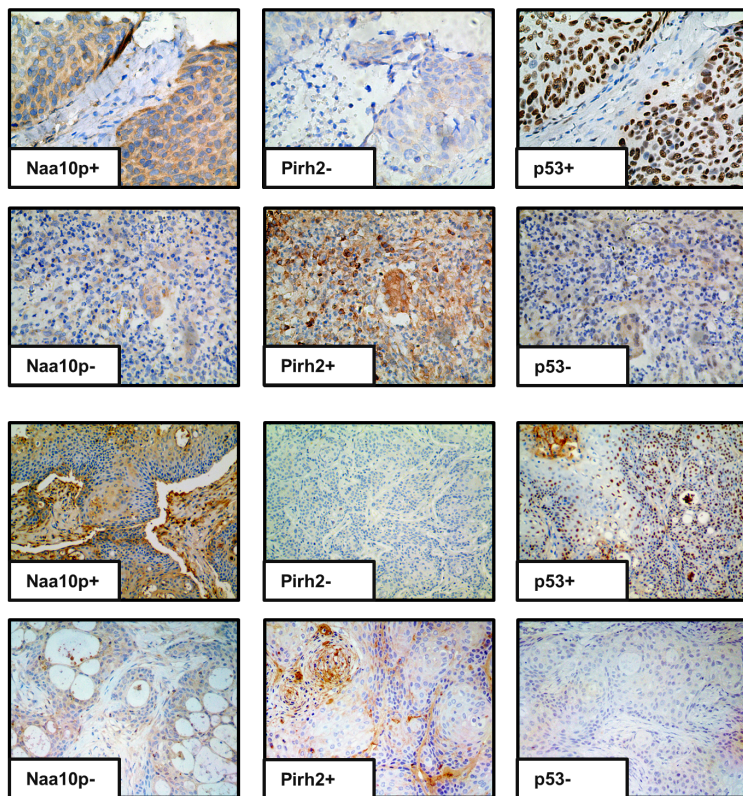


**Figure 2**

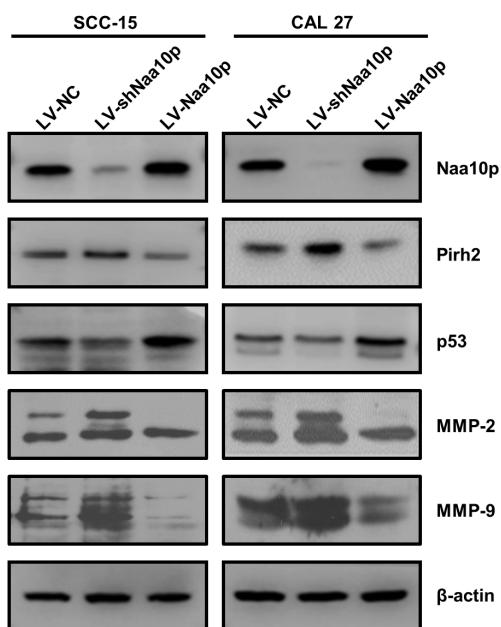
Naa10p expression level is closely associated with Pirh2-p53 signaling pathway. (a) Naa10p gene expression profile was analyzed after the stable interference of CAL 27 cells, and genes with differential expression of more than two folds were selected for KEGG analysis. The top 10 KEGG pathways were

displayed. (b) GSEA result showed that high Naa10p expression was positively correlated with p53 signaling in OSCC. NES, normalized enrichment score. (c) Differentially expressed genes of p53 signaling affected by Naa10p silencing in CAL 27 cells. The color intensity was proportional to the log<sub>2</sub> of expression ratio (blue, downregulated; red, upregulated). (d) Expression levels of selected genes in p53 pathway were examined by qRT-PCR in CAL 27 cells. Results were presented as the mean ± SD of three repeated experiments.

a



b



c

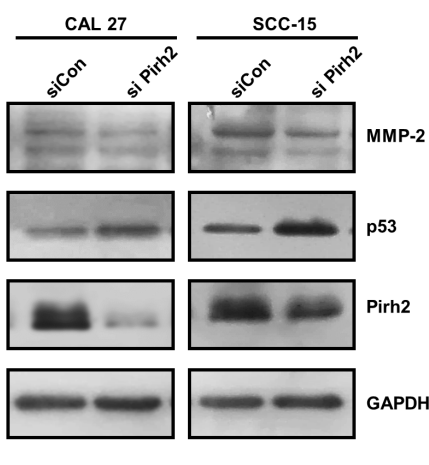
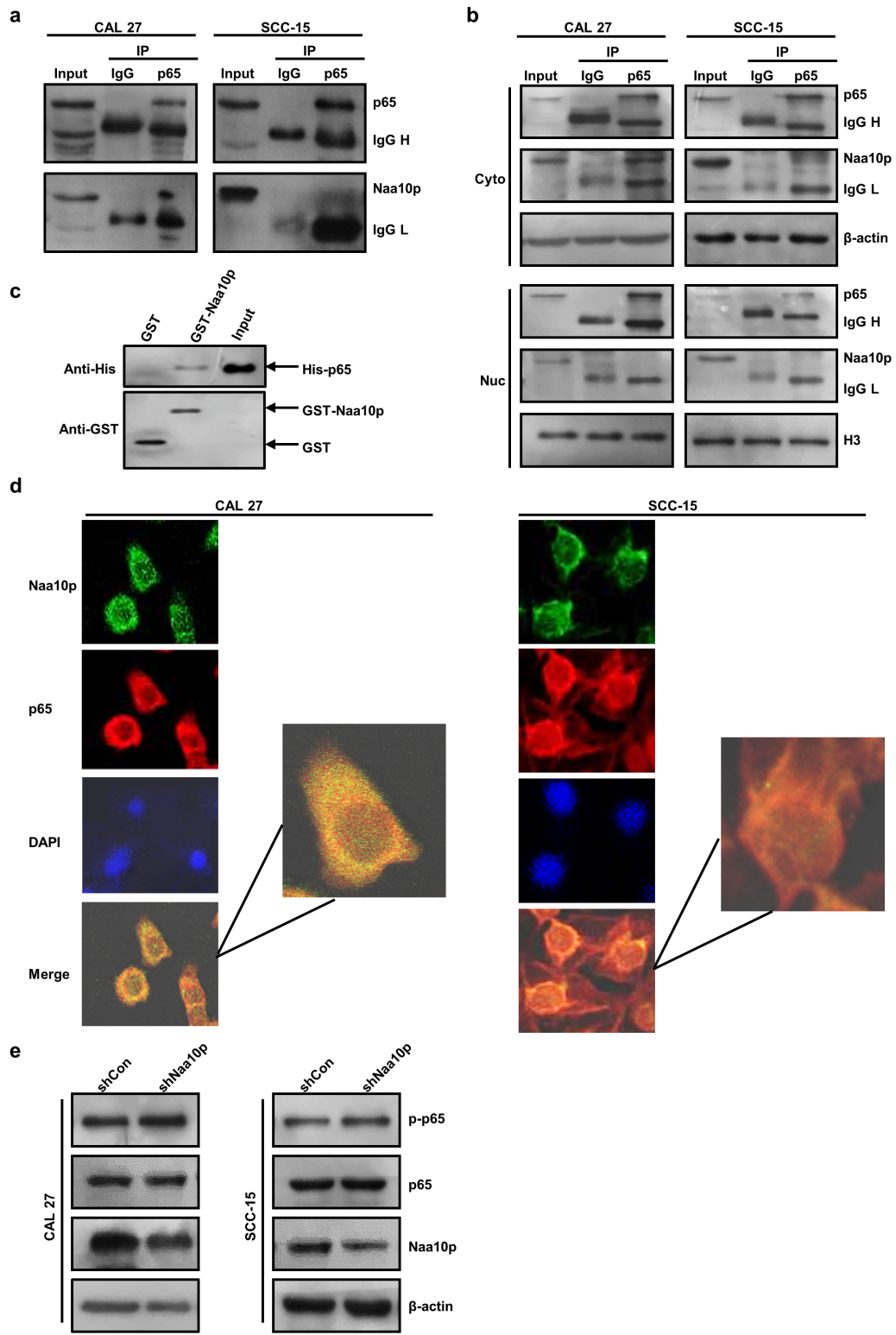


Figure 3

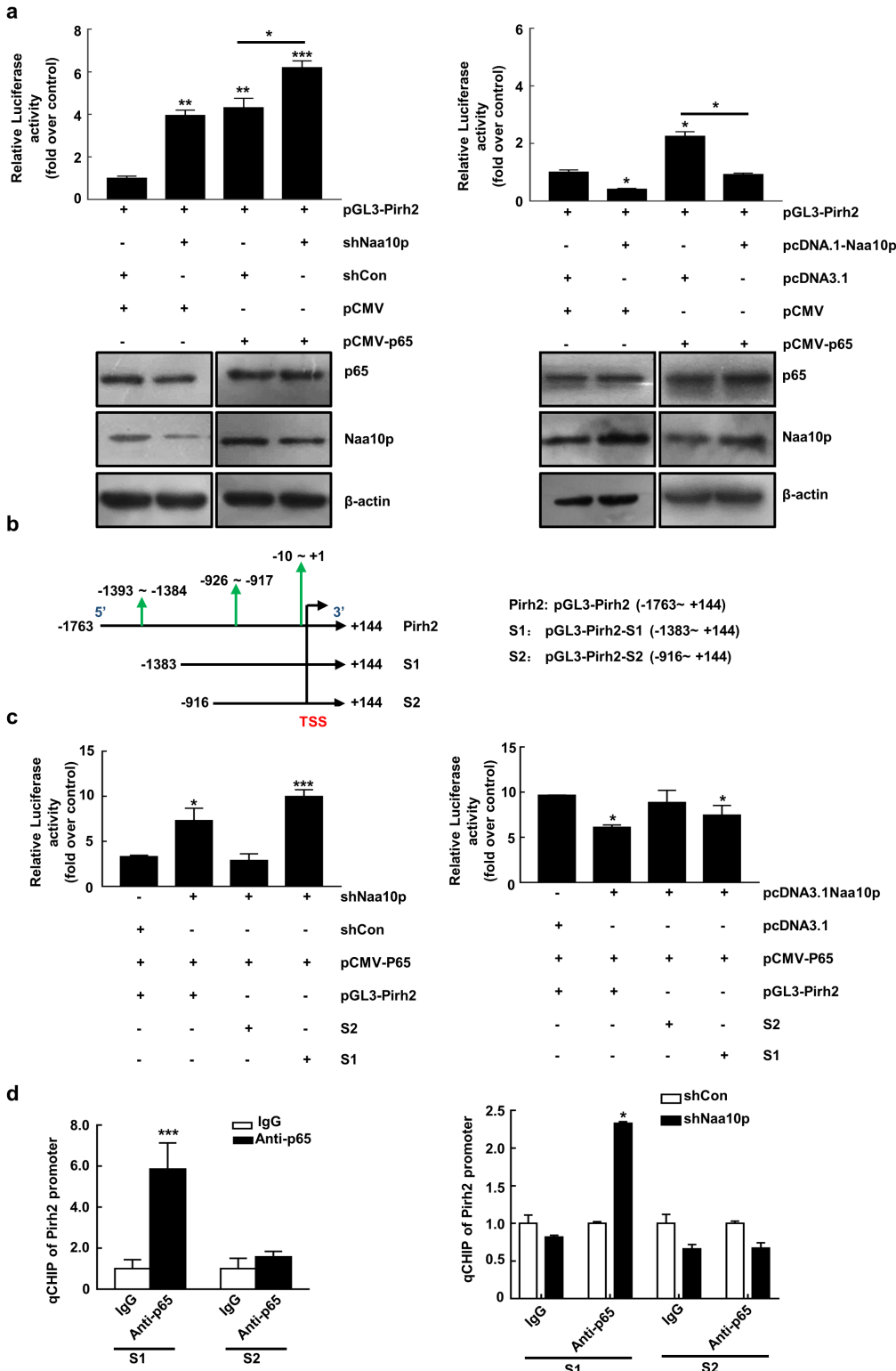
Naa10p regulates the expression of related proteins involved in the pirh2-p53 signaling. (a) Immunostaining of Naa10p, Pirh2, p53 in OSCC TMAs and tumor xenograft tissues. Two representative cases were shown. Magnification,  $\times 100$ . (b) Stable silencing of endogenous Naa10p increased expression of Pirh2, MMP2 and MMP9, but decreased p53. And stable expression of ectopic Naa10p decreased expression of Pirh2, MMP-2 and MMP-9, but increased p53 in indicated cells. (c) Endogenous Pirh2 expression in CAL 27 and SCC-15 cells was silenced by siRNA Scrambled siRNA (siCon) was used as a negative control. The effect of silencing Pirh2 on p53 and MMP-2 expression was detected by western blot.



**Figure 4**

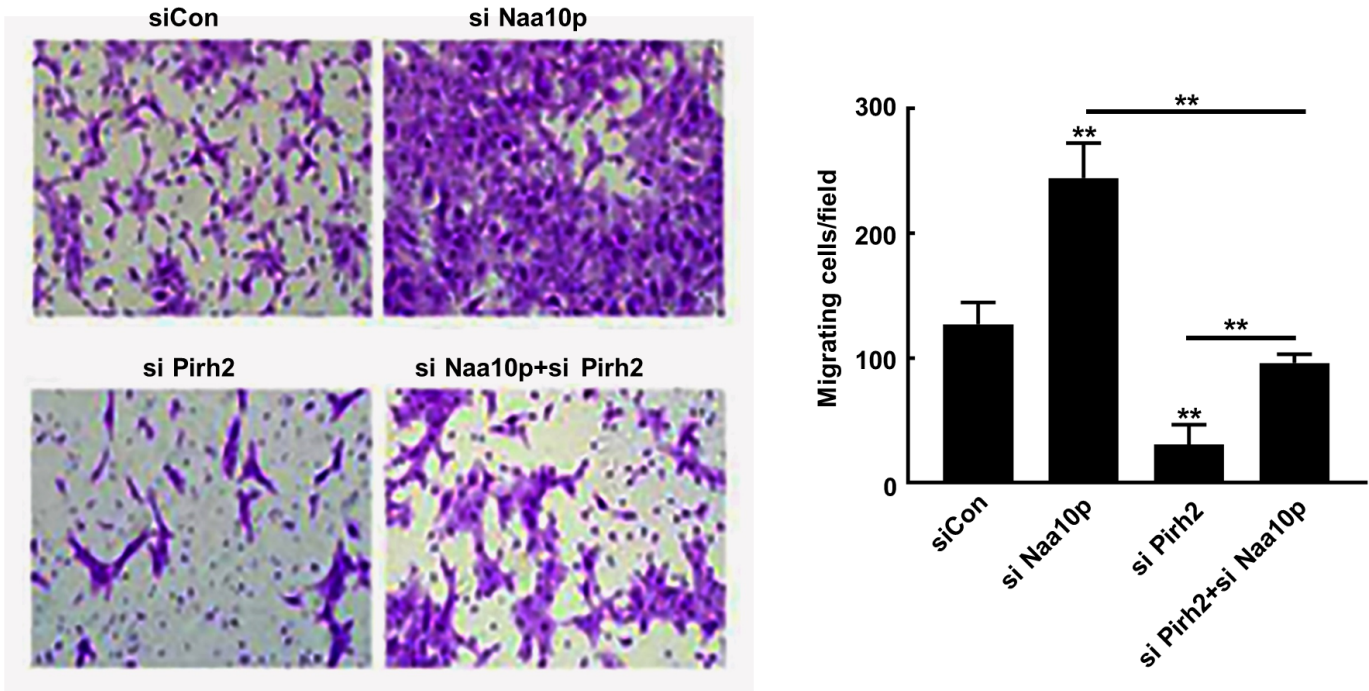
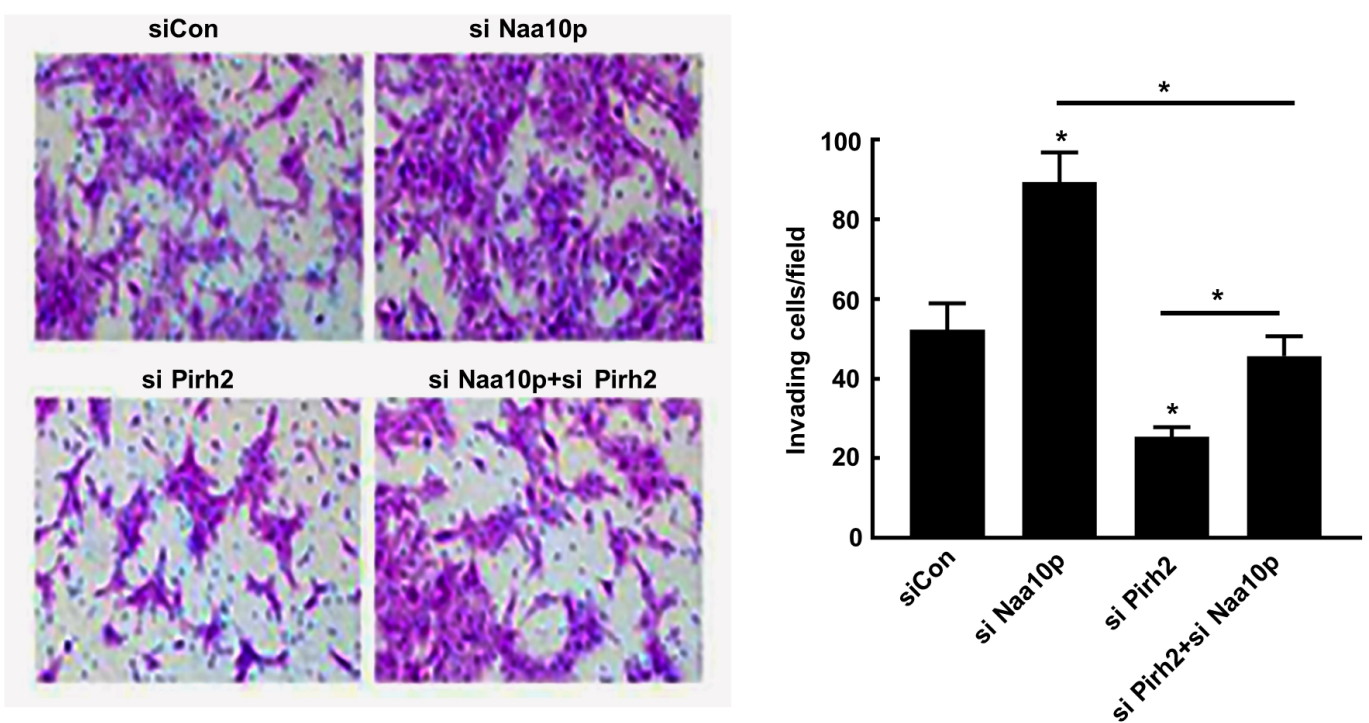
Naa10p is associated with RelA/p65 and influences the phosphorylation of p65. (a) Immunoprecipitation of Naa10p and RelA/p65 with an anti-RelA/p65 antibody in CAL 27 and SCC-15 cells. IgG H, IgG heavy chain; IgG L, IgG light chain. (b) Cytoplasmic and nuclear interactions between Naa10p and RelA/p65. Indicated cells were subjected to subcellular fractionation, and the qualities of cytoplasmic and nuclear extracts were, respectively, verified by western blot with antibodies against  $\beta$ -actin and H3. Cytoplasmic

protein (500 µg) and nuclear protein (200 µg) were immunoprecipitated with an anti-p65 antibody, followed by western blot with anti-Naa10p and anti-RelA/p65 antibodies. (c) Binding assay of His-p65 with GST or GST-Naa10p. (d) Colocalization of Naa10p and RelA/p65. CAL 27 and SCC-15 cells were subjected to immunofluorescence staining with anti-Naa10p (green) and anti-RelA/p65 (red) antibodies. Colocalization was shown by the merge (yellow). Nuclei were counterstained with 4',6-diamidino-2-phenylindole (DAPI) (blue). (e) shCon and shNaa10p were transfected into CAL 27 and SCC-15 cells, respectively. The endogenous level of p65 and p-p65 (Ser536) was detected by western blot.



## Figure 5

Naa10p suppressed RelA/p65-activated transcriptional expression of Pirh2. (a) Naa10p cooperated with RelA/p65 to regulate Pirh2 expression in luciferase assay. (b) According to transcription factor RelA/p65 binding sites in the Pirh2 promoter: site 1 (Pirh2p1), -1393 to -1384; and site 2 (Pirh2p2), -926 to - 917; and site 3 (Pirh2p3), - 10 to +1. Truncated Pirh2 promoter constructs were established. (c) Truncated Pirh2 promoter constructs were transfected to CAL 27 cells, respectively, and relative luciferase activities were determined. (d) CHIP-qPCR assay demonstrated the direct binding of RelA/p65 to the Pirh2 promoter. \*P < 0.05, \*\*\*P<0.005.

**a****b****Figure 6**

Pirh-p53 signaling pathway is indispensable for Naa10p mediated OSCC invasion and metastasis. (a) and (b) Transwell assays were used to evaluate whether Pirh2 knockdown blocked the promoting effects of silencing Naa10p on the migration (a) and invasion (b) of CAL 27 cells. \*P < 0.05, \*\*P < 0.01.

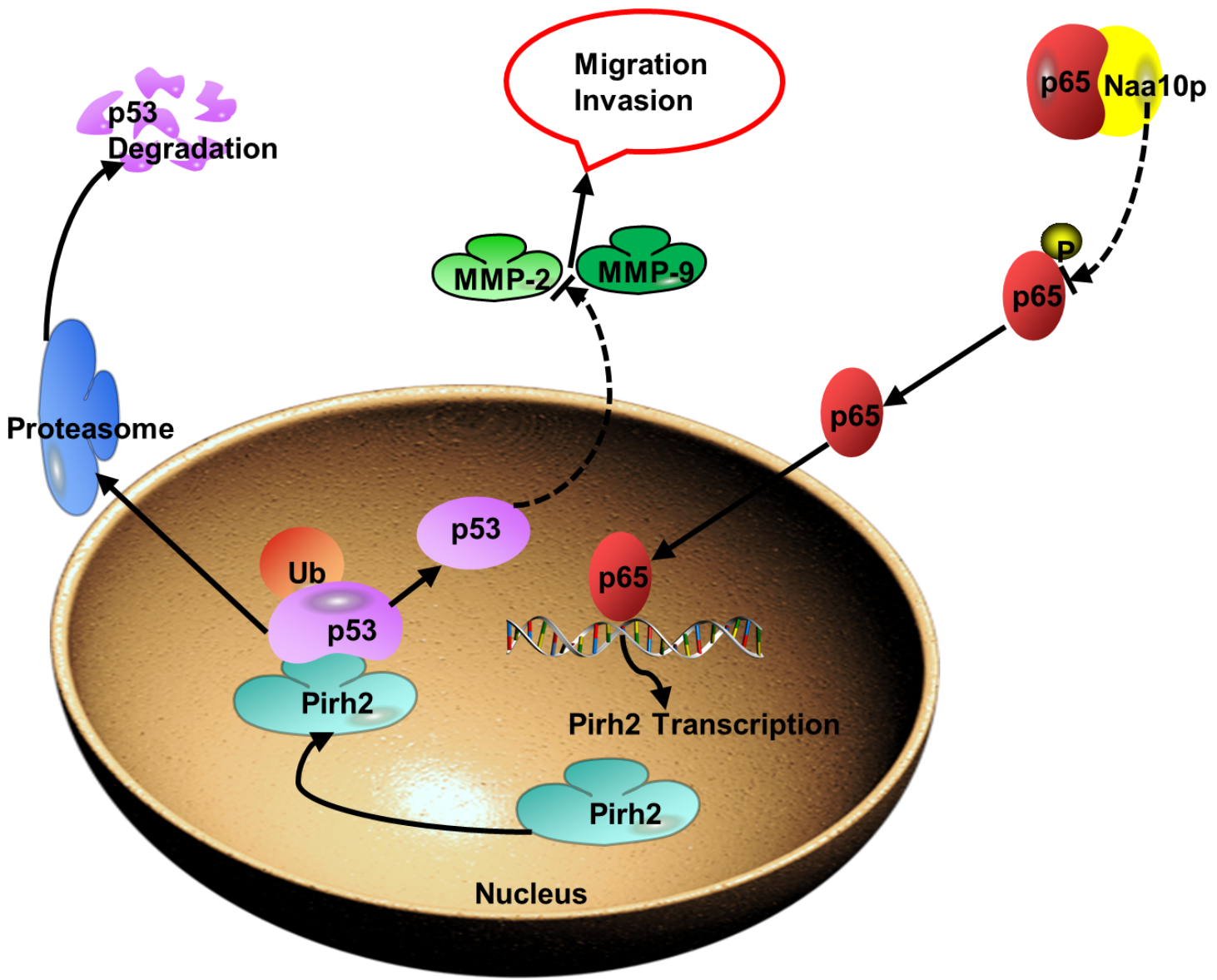


**Figure 7**

Schematic representation depicting the effects of Naa10p on OSCC invasion and metastasis. Naa10p, by interacting with p65 and inhibiting the phosphorylation of p65, inhibits p65 goes into the cell nucleus and binds to Pirh2 promoter, and further down-regulates the transcription expression of Pirh2 gene. Thereby the inhibition of Pirh2 increased the expression of the down-stream tumor suppressor genes p53, which leads to the down-regulation of the expression of the downstream MMP-2 and MMP-9 genes and plays the role of inhibiting the invasion and metastasis of oral squamous cell carcinoma cells.

## Supplementary Files

This is a list of supplementary files associated with this preprint. Click to download.

- [Supplementarymaterial.doc](#)